

SCIENTIFIC REPORTS



OPEN

Iridium-based probe for luminescent nitric oxide monitoring in live cells

Chun Wu¹, Ke-Jia Wu², Tian-Shu Kang², Hui-Min David Wang³, Chung-Hang Leung², Jin-Biao Liu^{1,4} & Dik-Lung Ma¹

Nitric oxide (NO) is an intra- and extracellular messenger with important functions during human physiology process. A long-lived luminescent iridium(III) complex probe **1** has been designed and synthesized for the monitoring of NO controllably released from sodium nitroprusside (SNP). Probe **1** displayed a 15-fold switch-on luminescence in the presence of SNP at 580 nm. The probe exhibited a linear response towards SNP between 5 to 25 μM with detection limit at 0.18 μM . Importantly, the luminescent switch-on detection of NO in HeLa cells was demonstrated. Overall, complex **1** has the potential to be applied for NO tracing in complicated cellular environment.

Nitric oxide (NO) plays an irreplaceable role in multiple processes of various physiology and pathology pathways, such as regulating vasodilatation, relaxation and immunization response, as well as the cardiovascular, peripheral and central nervous systems^{1–7}. Uncontrollable NO secretion is highly linked with the production of reactive nitrogen species (RNS) that can cause health issues including inflammation, endothelial dysfunction, neurodegeneration diseases or even cancer^{8,9}. However, the function mechanisms and complicated physiological involvement of NO are still not fully understood. The availability for rapid and selective NO monitoring turns out to be one of the key requirements for further investigation towards NO.

An attractive approach to detect NO in real time is with fluorescent probes¹⁰. A number of NO fluorescent organic probes have been developed for bioimaging^{11–13}, including a number of *o*-phenylenediamine-based probes by the group of Nagano (Table S1)^{14–16}. A frequently-used moiety for trapping NO is the electron-rich *o*-diaminophenyl functionality, as it is an effective quencher of fluorescence via photoinduced electron transfer (PET). Mechanistically, the reaction of NO with the *o*-diaminophenyl group under aerobic conditions forms the corresponding benzotriazole moiety, leading to the abrogation of PET quenching and the restoration of fluorescence¹⁷. However, although several NO probes based on organic dyes have been proposed¹⁸, the development of transition metal-based NO probes with advantageous characteristics, such as large Stokes shift, good photostability, long luminescence lifetime, and high intracellular retention^{19–23}, remains a challenge.

The Lippard group has developed several Cu(II)-based NO probes^{24–26}. The mechanism of these Cu(II)-based probes relies on the generation of a diamagnetic Cu(I) species triggered by NO reduction, which abolishes the fluorescence quenching accompanied with the paramagnetic Cu(II) center. Yuan's group has also reported an Eu(III) bearing luminescence probe that is selective towards NO²⁷. Additionally, an Ir(III) probe has been developed for endogenous NO imaging, which displayed good selectivity for NO tracking in the mitochondria of living cells²⁸.

Based on our current interest in the development of luminescent iridium(III) complex probes^{29–34}, we attempted to develop an iridium(III) complex platform for NO determination using SNP as the source of NO. We designed and synthesized an iridium(III) complex **1**, incorporating the *o*-diamine group in the phenanthroline N[^]N ligand, and with two 2-(*p*-tolyl)pyridine (tpy) units as C[^]N co-ligands. We envisioned that **1** could act as a NO probe through the reaction of the *o*-diamino groups with NO to form the triazole **2**. This reaction would inhibit the PET quenching effect from the *o*-diamino groups, leading to an increased switch-on response in the presence of NO (Fig. 1).

¹Department of Chemistry, Hong Kong Baptist University, Kowloon Tong, Hong Kong, China. ²State Key Laboratory of Quality Research in Chinese Medicine, Institute of Chinese Medical Sciences, University of Macau, Macao, China. ³Graduate Institute of Biomedical Engineering, National Chung Hsing University, Taichung, Taiwan, China. ⁴School of Metallurgical and Chemical Engineering, Jiangxi University of Science and Technology, Ganzhou, China. Correspondence and requests for materials should be addressed to J.-B.L. (email: liujbgood@hotmail.com) or D.-L.M. (email: edmondma@hkbu.edu.hk)

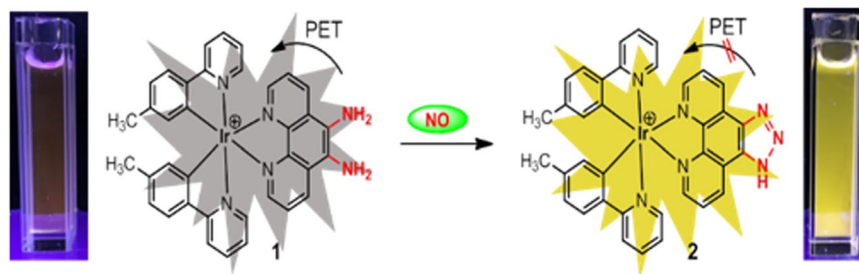


Figure 1. Mechanism of NO detection by complex **1**.

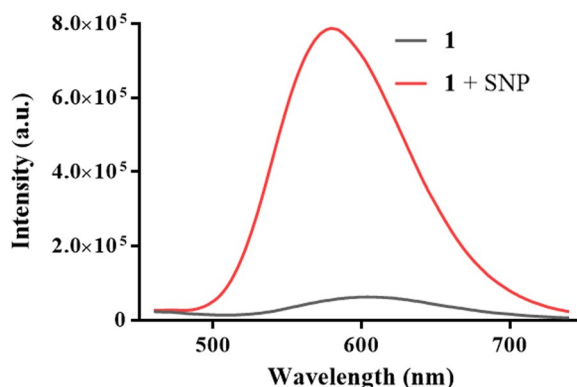


Figure 2. Emission spectra of complex **1** ($5\ \mu\text{M}$) in the absence and presence of SNP ($25\ \mu\text{M}$) in DMSO/PBS (9:1, v/v).

Results

Photophysical properties of complex 1. Complex **1** is readily generated from the organometallated dimer ($[\text{Ir}(\text{tpy})_2\text{Cl}]_2$) and 1,10-phenanthroline-5,6-diamine (Fig. S1). High resolution mass spectrometry (HRMS) and ^1H , ^{13}C NMR spectroscopy were employed for the characterization of complex **1** (Fig. S2). With complex **1** in hand, we next investigated the photophysical characteristics of complex **1**. Complex **1** exhibited a 265 ns lifetime (Table S2), which is typical of phosphorescence iridium(III) complexes, while organic dyes usually possess lifetimes within nanosecond regime. Importantly, the long lifetime of such iridium(III) scaffolds could allow them to be distinguished in autofluorescent samples via time-resolved luminescence spectroscopy (TRES). Moreover, **1** showed a maximal emission wavelength at 608 nm after excited at 355 nm, giving a calculated Stokes shift for about 253 nm (Table S2), which is much greater than the Stokes shifts generally shown by organic dyes.

Signal response of **1 to NO.** As endogenous NO production is usually uncontrollable and ambiguous in certain cases, an exogenous NO source such as sodium nitroprusside (SNP)^{35,36} is commonly used to understand the role of NO in pathologic and physiologic pathways. We initially investigated the emission response of **1** towards NO generated from SNP after UV light irradiation for one minute. In the absence of SNP, **1** displayed very weak luminescence in a 9:1 blend of dimethyl sulfoxide (DMSO) and PBS buffer (50 mM, pH = 7.4). However, upon the addition of SNP, the luminescence signal of **1** was enhanced significantly by around 15-fold (Fig. 2), which was largely attributed to the accelerated release of NO from SNP under UV light³⁷.

We next investigated the luminescent behavior of **1** to SNP in solvent systems containing various proportions of DMSO and PBS buffer. Our probe displayed the most significant luminescence enhancement in DMSO/buffer (9:1, v/v), whereas the luminescence response of the probe was decreased as the percentage of DMSO in solution was reduced (Fig. S3). We also examined other organic solvents such as DMSO, dimethyl formamide (DMF), acetonitrile (ACN), acetone, tetrahydrofuran (THF), ethanol (EtOH) and methanol (MeOH) for the detection system (with 10% PBS buffer solution) and discovered that DMSO offered the most optimal probe response (Fig. S4). In an emission titration experiment, complex **1** ($5\ \mu\text{M}$) displayed an increasing luminescence intensity with increasing concentration of SNP (Fig. 3a). A linear correlation ($R^2 = 0.980$) was observed from 5 to $25\ \mu\text{M}$ of SNP, and a detection limit of $0.18\ \mu\text{M}$ was measured (Fig. 3b) based on the 3σ method. To validate the reaction-based mechanism of the assay, HRMS analysis was performed on the reaction mixture. The results indicated the production of triazole **2** at $m/z = 750.1918$ (expected m/z : 750.1952), suggesting that the reaction between complex **1** with NO took place (Fig. S5). Complex **2** exhibited a maximum emission wavelength at 584 nm, which represented a blue shift of 24 nm compared to complex **1** (608 nm). Importantly, complex **2** showed much stronger luminescence intensity compared to complex **1**. Moreover, complex **2** showed a stronger UV-Vis absorbance profile and a longer luminescence lifetime compared to complex **1** (Fig. S6).

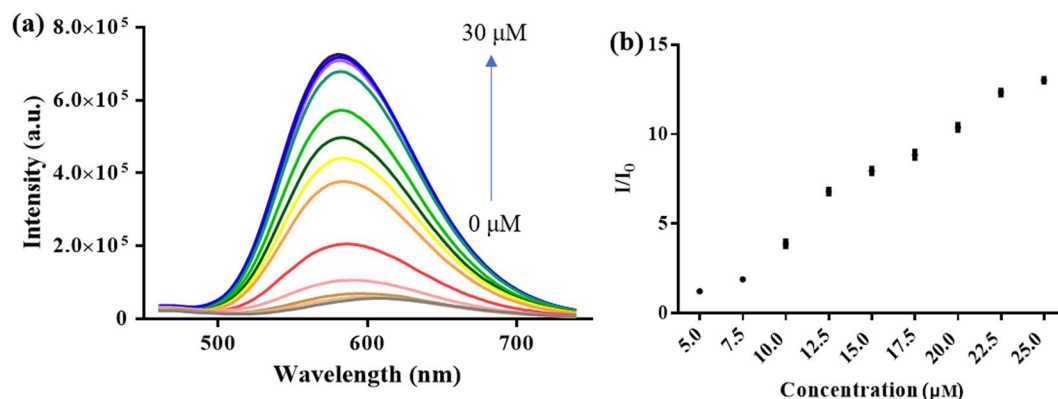


Figure 3. (a) Luminescence spectra of complex **1** ($5\ \mu\text{M}$) in DMSO/PBS buffer (9:1, v/v, 50 mM, pH = 7.4) with increasing concentration of SNP: 0, 2.5, 5.0, 7.5, 10.0, 12.5, 15.0, 17.5, 20.0, 22.5, 25.0, 27.5, 30.0 μM). (b) Luminescence enhancement ratio of complex **1** upon increasing SNP concentration.

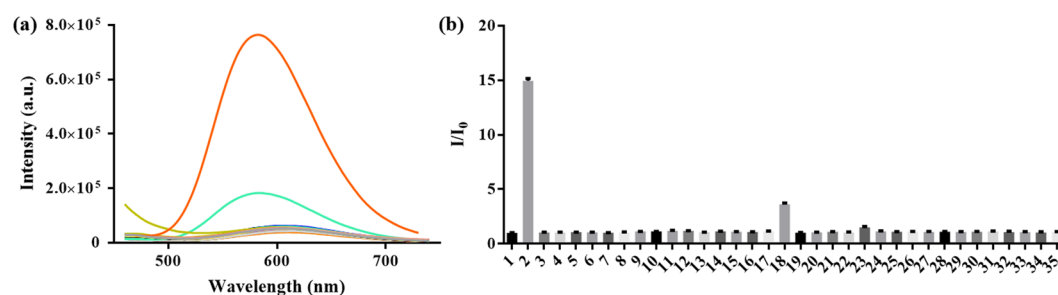


Figure 4. (a) Luminescence intensity change at 580 nm in the presence of various targets: (1) complex **1** ($5\ \mu\text{M}$), (2) SNP, (3) Met, (4) Pro, (5) Trp, (6) Val, (7) Ala, (8) Asp, (9) Tyr, (10) Arg, (11) Glu, (12) Cys, (13) GSH, (14) Mg^{2+} , (15) Na^+ , (16) Ca^{2+} , (17) NO_3^- , (18) NO_2^- , (19) H_2O_2 , (20) HClO , (21) Lys, (22) Gly, (23) His, (24) Phe, (25) Leu, (26) Asn, (27) Ile, (28) Ser, (29) Thr, (30) Gln, (31) Cl^- , (32) CO_3^{2-} , (33) HCO_3^- , (34) HPO_4^{2-} , (35) H_2PO_4^- . $\lambda_{\text{ex}} = 355\ \text{nm}$. (b) The bars show the relative luminescence intensity change of complex **1** and further addition of various interferences at 580 nm.

Selectivity of complex 1 for NO. The selectivity of **1** ($5\ \mu\text{M}$) for SNP was tested over other possible biologically relevant species (25 μM), including reactive oxygen species (H_2O_2 and HClO), nitrogen species (NO_2^- and NO_3^-), amino acids (Cys, GSH, Glu, Arg, Tyr, Asp, Tyr, Val, Trp, Pro, Ala, Met, Lys, Gly, His, Phe, Leu, Asn, Ile, Ser, Thr and Gln), metal ions (Na^+ , Mg^{2+} and Ca^{2+}) and anions (Cl^- , CO_3^{2-} , HCO_3^- , HPO_4^{2-} , H_2PO_4^-). Negligible luminescence response of **1** toward these species were observed, with the exception of NO_2^- which produced a 3-fold intensity enhancement (Fig. 4). In contrast, only SNP displayed a very strong turn-on luminescence at 580 nm, indicating the high selectivity of **1** towards SNP. This selectivity could be attributed to the unique reaction between the *o*-diamine functionality of **1** with NO, producing the triazole unit. The high selectivity of complex **1** for NO renders it as a reliable probe for tracing NO in physiological environments.

Application of SNP detection assay in live cells. Encouraged by the performance of complex **1** for the *in vitro* detection of SNP, the cytotoxicity of complex **1** was measured in HeLa cells and normal liver LO2 cells (Fig. S7). The results revealed that complex **1** exhibited negligible toxicity towards either HeLa cells or LO2 cells at 100 μM . This indicates that complex **1** is relatively nontoxic to cells, making it suitable for cell imaging applications.

We next explored whether complex **1** could be employed for the tracing of NO in HeLa cells. Upon the addition of complex **1** (10 μM) only or SNP (100 μM) only, no significant luminescence could be observed (Fig. 5) even after UV light irradiation for 10 min. However, a strong yellow luminescence could be observed in the presence of both complex **1** and SNP under the same condition. This suggests that complex **1** could be used to image NO in living cells, with the further potential to demonstrate the involvement of NO in cellular reactions. In order to examine the accumulation of complex **1** in cells, an inductively-coupled plasma mass spectrometry (ICP-MS) assay was performed (Fig. S8). As shown in Fig. S8, HeLa cells incubated with complex **1** showed a significant enhancement of iridium content in the cellular environment, suggesting the successful transportation of complex **1** into HeLa cells.

Considering the feasibility for intracellular sensing of NO using complex **1**, the intracellular response of complex **1** upon addition of different concentrations of SNP (0–100 μM) was further investigated. As shown in Fig. S9, HeLa cells displayed a luminescence that was mainly generated in cytoplasm at lower concentrations of SNP (10–50 μM). However, upon increasing of SNP concentration to 100 μM , a detectable luminescence generated

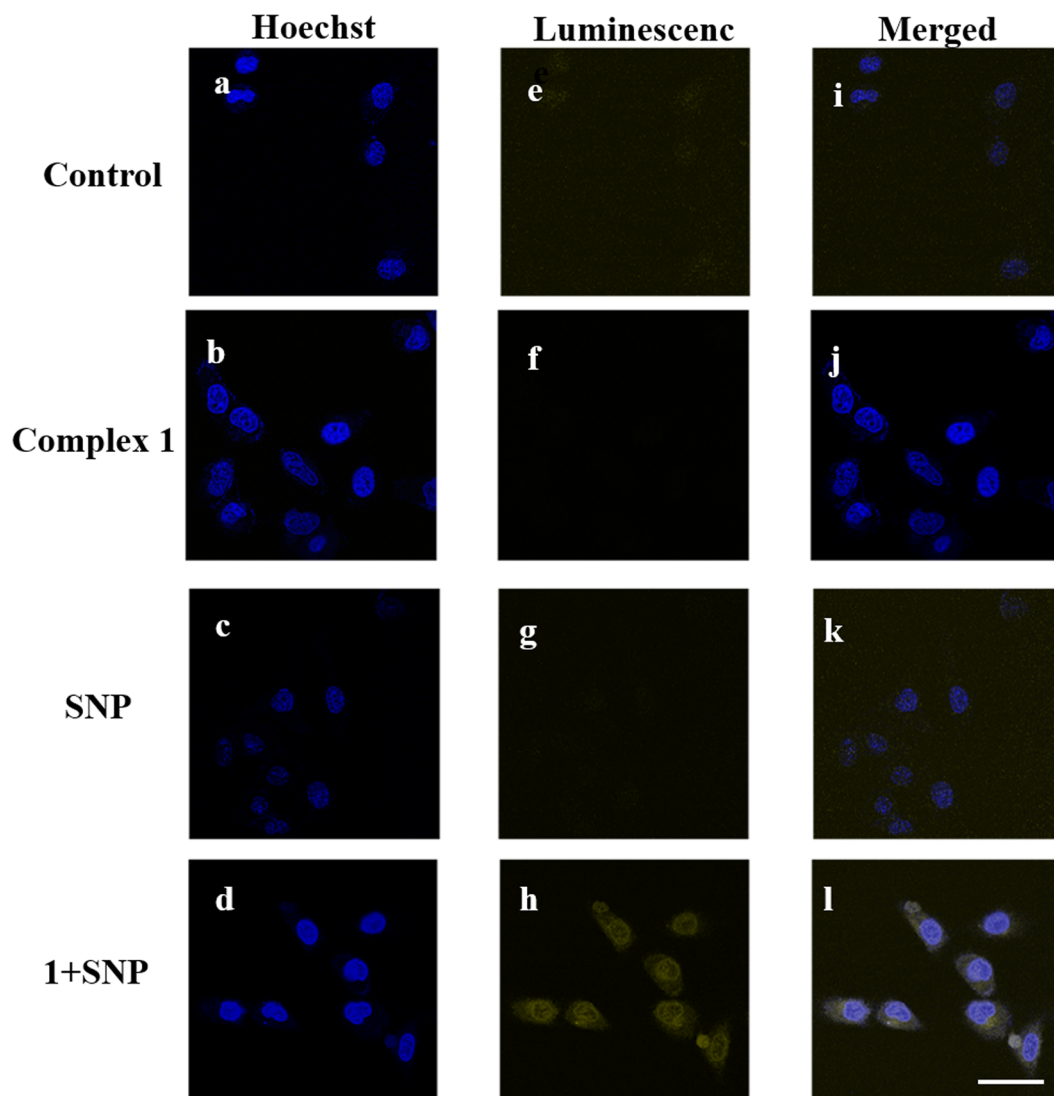


Figure 5. Confocal imaging of HeLa cells incubated with complex **1** ($10\ \mu\text{M}$) with SNP ($100\ \mu\text{M}$) for 3 h at 37°C and UV irradiation for 10 min. Excitation was at 405 nm, and luminescence images were recorded from 570 to 640 nm. Nuclei were stained with $5\ \mu\text{g}/\text{mL}$ Hoechst for 5 min. The scale bar is $50\ \mu\text{m}$.

from complex **1** could also be observed in the nuclear area, suggesting that higher concentrations of SNP might facilitate detectable NO monitoring in both the cytoplasm and nucleus of HeLa cells.

Moreover, the intracellular luminescence intensities of HeLa cells treated with complex **1** ($10\ \mu\text{M}$) and SNP ($100\ \mu\text{M}$) for different times (1, 3 and 6 h) were monitored using fluorescent microscopy (Fig. S10). The luminescence of the cells increased over time and was predominantly localized in the cytoplasm at 1 h, before spreading to the whole cell at 3 and 6 h, indicating the feasibility for NO detection within 6 h in the cellular environment.

Discussion

In this paper, we have successfully designed and synthesized an iridium(III) probe **1** and used it as a turn-on chemosensor for NO monitoring. **1** bears an *o*-diamine group in the $\text{N}^{\wedge}\text{N}$ donor ligand, which allows it to act as a recognition unit for NO. In the presence of SNP, **1** experienced about 15-fold emission increase at 580 nm. Compared with typical organic dyes, **1** displayed a long lifetime luminescence and a wide Stokes shift. We expect that probe **1** could offer a versatile scaffold for assisting the mechanism investigations of NO in biological processes.

Methods

Nitric oxide detection. Sodium nitroprusside (SNP) was dissolved in water to achieve a 1 M stock concentration. Afterwards, different concentrations of SNP were added to DMSO/PBS buffer (9:1, v/v, pH = 7.4) containing complex **1** ($5\ \mu\text{M}$) in a cuvette for 1 min irradiation under UV light at 365 nm. Luminescence emission spectra were recorded on a PTI QM-1 spectrofluorometer (Photo Technology International, Birmingham, NJ) at 25°C , with the slits for both excitation and emission set at 2.5 nm. UV-Vis absorption spectra were recorded on a Cary UV-300 spectrophotometer (double beam).

Confocal imaging. Cells were seeded into a glass-bottomed dish (35 mm dish with 20 mm well). After 12 h, cells were incubated with complex **1** and SNP for the indicated time periods or concentrations, followed by UV light irradiation for 10 min and further washing with phosphate-buffered saline three times. The luminescence imaging of complexes in cells was carried out by a Leica TCS SP8 confocal laser scanning microscope system. The excitation wavelength was 405 nm.

References

- Snyder, S. H. Nitric oxide: first in a new class of neurotransmitters? *Science* **257**, 494–496 (1992).
- Klionsky, D. J. & Emr, S. D. Autophagy as a regulated pathway of cellular degradation. *Science* **290**, 1717–1721 (2000).
- Shintani, T. & Klionsky, D. J. Autophagy in health and disease: a double-edged sword. *Science* **306**, 990–995 (2004).
- Sarkar, S. *et al.* Complex inhibitory effects of nitric oxide on autophagy. *Mol. Cell* **43**, 19–32 (2011).
- Rabinowitz, J. D. & White, E. Autophagy and metabolism. *Science* **330**, 1344–1348 (2010).
- Xie, Z. & Klionsky, D. J. Autophagosome formation: core machinery and adaptations. *Nat. Cell Biol.* **9**, 1102 (2007).
- Fukumura, D., Kashiwagi, S. & Jain, R. K. The role of nitric oxide in tumour progression. *Nat. Rev. Cancer* **6**, 521 (2006).
- Moncada, S., Palmer, R. & Higgs, E. A. Nitric oxide: physiology, pathophysiology, and pharmacology. *Pharmacol. Rev.* **43**, 109–142 (1991).
- Pacher, P., Beckman, J. S. & Liaudet, L. Nitric oxide and peroxynitrite in health and disease. *Physiol. Rev.* **87**, 315–424 (2007).
- Zhou, X., Lee, S., Xu, Z. & Yoon, J. Recent progress on the development of chemosensors for gases. *Chem. Rev.* **115**, 7944–8000 (2015).
- Nagano, T. & Yoshimura, T. Bioimaging of nitric oxide. *Chem. Rev.* **102**, 1235–1270 (2002).
- Chen, X., Tian, X., Shin, I. & Yoon, J. Fluorescent and luminescent probes for detection of reactive oxygen and nitrogen species. *Chem. Soc. Rev.* **40**, 4783–4804 (2011).
- Dong, X., Heo, C. H., Chen, S., Kim, H. M. & Liu, Z. Quinoline-based two-photon fluorescent probe for nitric oxide in live cells and tissues. *Anal. Chem.* **86**, 308–311 (2013).
- Hirano, T., Kikuchi, K., Urano, Y., Higuchi, T. & Nagano, T. Novel zinc fluorescent probes excitable with visible light for biological applications. *Angew. Chem. Int. Ed.* **112**, 1094–1096 (2000).
- Gabe, Y., Urano, Y., Kikuchi, K., Kojima, H. & Nagano, T. Highly sensitive fluorescence probes for nitric oxide based on boron dipyrromethene chromophore rational design of potentially useful bioimaging fluorescence probe. *J. Am. Chem. Soc.* **126**, 3357–3367 (2004).
- Sasaki, E. *et al.* Highly sensitive near-infrared fluorescent probes for nitric oxide and their application to isolated organs. *J. Am. Chem. Soc.* **127**, 3684–3685 (2005).
- Kojima, H. *et al.* Detection and imaging of nitric oxide with novel fluorescent indicators: diaminofluoresceins. *Anal. Chem.* **70**, 2446–2453 (1998).
- Li, H. & Wan, A. Fluorescent probes for real-time measurement of nitric oxide in living cells. *Analyst* **140**, 7129–7141 (2015).
- Huang, T., Yu, Q., Liu, S., Huang, W. & Zhao, Q. Phosphorescent iridium (III) complexes: a versatile tool for biosensing and photodynamic therapy. *Dalton Trans.* **47**, 7628–7633 (2018).
- Chen, Z. *et al.* Phosphorescent polymeric thermometers for *in vitro* and *in vivo* temperature sensing with minimized background interference. *Adv. Funct. Mater.* **26**, 4386–4396 (2016).
- Liu, S. *et al.* Time-resolved luminescence imaging of intracellular oxygen levels based on long-lived phosphorescent iridium (III) complex. *Opt. Express* **24**, 15757–15764 (2016).
- Liu, S. *et al.* Phosphorescent ion-paired iridium (III) complex for ratiometric and time-resolved luminescence imaging of intracellular biothiols. *Opt. Express* **24**, 28247–28255 (2016).
- Zhao, Q. *et al.* Dual-emissive Polymer Dots for Rapid Detection of Fluoride in Pure Water and Biological Systems with Improved Reliability and Accuracy. *Sci. Rep.* **5**, 16420 (2015).
- Lim, M. H., Xu, D. & Lippard, S. J. Visualization of nitric oxide in living cells by a copper-based fluorescent probe. *Nat. Chem. Biol.* **2**, 375 (2006).
- Lim, M. H. *et al.* Direct nitric oxide detection in aqueous solution by copper (II) fluorescein complexes. *J. Am. Chem. Soc.* **128**, 14364–14373 (2006).
- Lim, M. H. & Lippard, S. J. Metal-based turn-on fluorescent probes for sensing nitric oxide. *Acc. Chem. Res.* **40**, 41–51 (2007).
- Chen, Y., Guo, W., Ye, Z., Wang, G. & Yuan, J. A europium (III) chelate as an efficient time-gated luminescent probe for nitric oxide. *Chem. Commun.* **47**, 6266–6268 (2011).
- Chen, X. *et al.* A fast and selective two-photon phosphorescent probe for the imaging of nitric oxide in mitochondria. *Biomaterials* **58**, 72–81 (2015).
- Liu, J.-B. *et al.* A long lifetime iridium (III) complex as a sensitive luminescent probe for bisulfite detection in living zebrafish. *Sens. Actuators. B Chem.* **243**, 971–976 (2017).
- Wu, C. *et al.* A reaction-based luminescent switch-on sensor for the detection of OH⁻ ions in simulated wastewater. *Dalton Trans.* **46**, 6677–6682 (2017).
- Ma, D.-L., Lin, S., Wang, W., Yang, C. & Leung, C.-H. Luminescent chemosensors by using cyclometalated iridium (III) complexes and their applications. *Chem. Sci.* **8**, 878–889 (2017).
- Liu, J.-B. *et al.* An aldol reaction-based Iridium (III) chemosensor for the visualization of proline in living cells. *Sci. Rep.* **6**, 36509 (2016).
- Vellaisamy, K. *et al.* Cell imaging of dopamine receptor using agonist labeling iridium (III) complex. *Chem. Sci.* **9**, 1119–1125 (2018).
- Liu, L.-J. *et al.* Inhibition of the Ras/Raf interaction and repression of renal cancer xenografts *in vivo* by an enantiomeric iridium (III) metal-based compound. *Chem. Sci.* **8**, 4756–4763 (2017).
- Grossi, L. & D'Angelo, S. Sodium Nitroprusside: Mechanism of NO Release Mediated by Sulfhydryl-Containing Molecules. *J. Med. Chem.* **48**, 2622–2626 (2005).
- Bates, J. N., Baker, M. T., Guerra, R. Jr. & Harrison, D. G. Nitric oxide generation from nitroprusside by vascular tissue: evidence that reduction of the nitroprusside anion and cyanide loss are required. *Biochem. Pharmacol.* **42**, S157–S165 (1991).
- Allardyce, C. S. & Dyson, P. J. Ruthenium in medicine: current clinical uses and future prospects. *Platin. Met. Rev.* **45**, 62–69 (2001).

Acknowledgements

This work is supported by Hong Kong Baptist University (FRG2/16-17/007, FRG2/17-18/003), the Health and Medical Research Fund (HMRF/14150561), the Research Grants Council (HKBU/12301115), the National Natural Science Foundation of China (21575121, 21775131, 21628502), the Hong Kong Baptist University Century Club Sponsorship Scheme 2018, the Interdisciplinary Research Matching Scheme (RC-IRMS/15-16/03), Innovation and Technology Fund (ITS/260/16FX), Collaborative Research Fund (C5026-16G), Matching Proof of Concept Fund (MPCF-001-2017/18), the Science and Technology Development Fund, Macao SAR (077/2016/A2), the University of Macau (MYRG2016-00151-ICMS-QRCM), and the Natural Science Foundation of Jiangxi Province (20171BAB213008).

Author Contributions

C. Wu, K.-J. Wu and T.-S. Kang carried out all the experiments, performed the data analysis and wrote the manuscript. Dr. J.-B. Liu assisted in experimental process and manuscript writing throughout the project. Dr. D.-L. Ma, Prof. C.-H. Leung and Prof. H.-M. Wang supervised the experiments and analyzed the results.

Additional Information

Supplementary information accompanies this paper at <https://doi.org/10.1038/s41598-018-30991-9>.

Competing Interests: The authors declare no competing interests.

Publisher's note: Springer Nature remains neutral with regard to jurisdictional claims in published maps and institutional affiliations.



Open Access This article is licensed under a Creative Commons Attribution 4.0 International License, which permits use, sharing, adaptation, distribution and reproduction in any medium or format, as long as you give appropriate credit to the original author(s) and the source, provide a link to the Creative Commons license, and indicate if changes were made. The images or other third party material in this article are included in the article's Creative Commons license, unless indicated otherwise in a credit line to the material. If material is not included in the article's Creative Commons license and your intended use is not permitted by statutory regulation or exceeds the permitted use, you will need to obtain permission directly from the copyright holder. To view a copy of this license, visit <http://creativecommons.org/licenses/by/4.0/>.

© The Author(s) 2018